CHAPTER 17

Design of support structures for offshore wind turbines

J. van der Tempel, N.F.B. Diepeveen, D.J. Cerda Salzmann & W.E. de Vries
Department of Offshore Engineering, Delft University of Technology, The Netherlands.

Offshore wind is the logical next step in the development of wind energy. With higher wind speeds offshore and the fact that turbines can be placed out of sight, offshore wind helps increase the amount of renewable energy significantly. Offshore wind has been developed through pilot projects in the 1990s and has seen commercial development over the last decade. This chapter shows the development of offshore wind and then focuses on the design of support structures. It briefly describes all fundamental steps that need to be taken to come to a proper support structure design, incorporating all turbine loads and the impact of waves and soil. Furthermore, the chapter gives an overview of the different types of structures and how they are fabricated and installed.

1 Introduction

As wind energy developed on land, the locations with a favourable wind climate became scarce, but the demand for clean energy still grew. The solution for many countries lies at their doorstep: offshore. Around the world, many densely populated areas are close to the sea. Offshore, the wind blows stronger and more constant, unhindered by obstacles. This led to the development of offshore wind farms: turbines placed at sea.

This chapter describes the design of offshore wind turbines. Turbine design for offshore follows the general design approach for onshore, although typical load cases are somewhat different and the turbine needs to withstand the more severe environment: salt. The structures on which the turbines are placed are significantly different, though. Different from their onshore counterparts but also from other

WIT Transactions on State of the Art in Science and Engineering, Vol 44, © 2010 WIT Press
www.witpress.com, ISSN 1755-8336 (on-line)
doi:10.2495/978-1-84564-205-1/17

structures found at sea. The design is not only dependent on turbine loads and associated overturning moment, the wave and currents add significant loads too. For the design of these structures wind, wave and current loads need to be assessed as acting on the offshore wind turbine system as a whole.

The development of offshore wind began in the 1970s and 1980s with studies and assessment of the potential wind resource offshore. In the 1990s several pilot offshore wind farms were constructed in the European waters, which helped develop knowledge and new technology. In 2002, the first large offshore wind farm Horns Rev was constructed in the North Sea off the Danish coast: 80 turbines with an installed capacity of 160 MW. In the years that followed, other countries followed with the construction of these large, commercial offshore wind farms. The EU target for 2020 is to have 40 GW of installed capacity.

2 History of offshore, wind and offshore wind development of offshore structures

2.1 The origin of "integrated design" in offshore wind energy

During the 1970s, 1980s and early 1990s, a number of studies were conducted in the field of offshore wind energy. Offshore and shipbuilding as well as renewable energy groups drafted reports on how to effectively harness the offshore wind energy potential. The first designs were mainly based on the multi-megawatt prototype turbines built in the 1970s: 3 MW and more. The structures were large, heavy and stiff: based on the accumulated experience of offshore construction in the North Sea for oil & gas exploitation. Figure 1 shows examples of a design from the British RES study and a Heerema tripod design [1, 2].

The design did incorporate combined wind and wave loading, but only on a basic level for extreme load case calculations. The stiffness of the structure prevented heavy dynamic response, so fatigue was not a big issue. For the subject operation and maintenance a direct copy of offshore platforms was made: the addition of a complete helicopter deck.

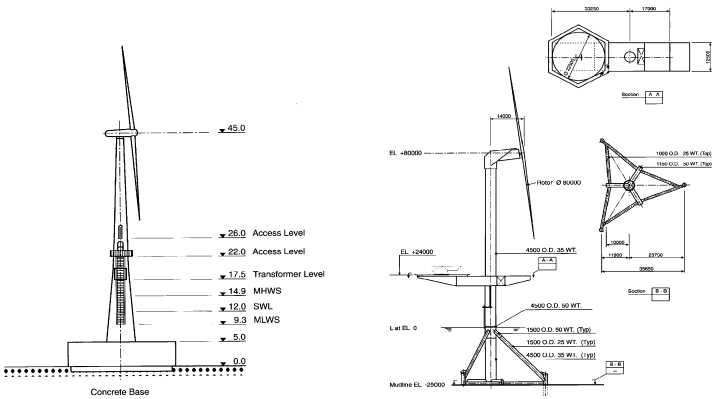

Figure 1: Offshore wind turbine design from the RES and the Heerema study.

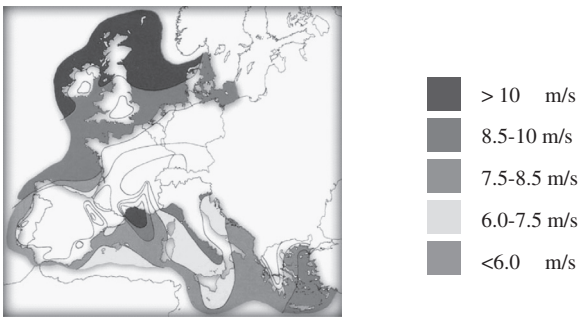

Figure 2: Yearly average wind speed at 100 m height for the European Seas.

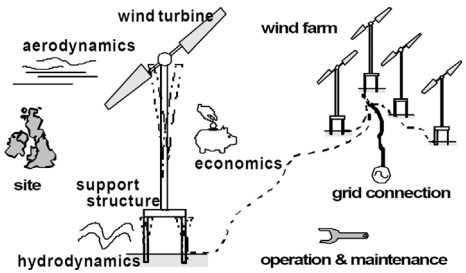

Figure 3: Subjects covered in the integrated design approach of the Opti-OWECS study.

In 1995 the Joule I "Study of Offshore Wind Energy in the EC" was published [3]. The study gave an overview of the wind potential offshore as shown in Fig. 2. The study described the design of offshore wind turbines in a more generic way with example designs for different types of offshore wind turbines. It was found that for one turbine wave loads could be dominant while for the other wind was the dominant load source. One of the main issues found was the benefit of aerodynamic damping on the dynamic behaviour of the structure when the turbine is in operation. It was also stated that a softer support structure would further enhance the aerodynamic damping effect, but at the cost of increased tower motion.

The Joule III Opti-OWECS [1] report finally made a complete design focusing on the integrated dynamic features of flexible offshore wind turbines. The design incorporated the entire offshore wind farm with all its features from turbines to operation and maintenance philosophy to cost modelling. Figure 3 gives an overview of all subjects covered in this integrated design scheme.

The Opti-OWECS study further explored the possibilities of flexible dynamic design. Although several types of support structures were reviewed, it was decided to make a full design of a soft monopile structure to benefit in full from the aerodynamic damping and assess the potential negative consequences of large structural motion. It was found that a structure could be designed with a natural frequency below both the rotation and the blade passing frequency of the turbine, a so-called soft–soft structure. The frequency distributions are shown in Fig. 4.

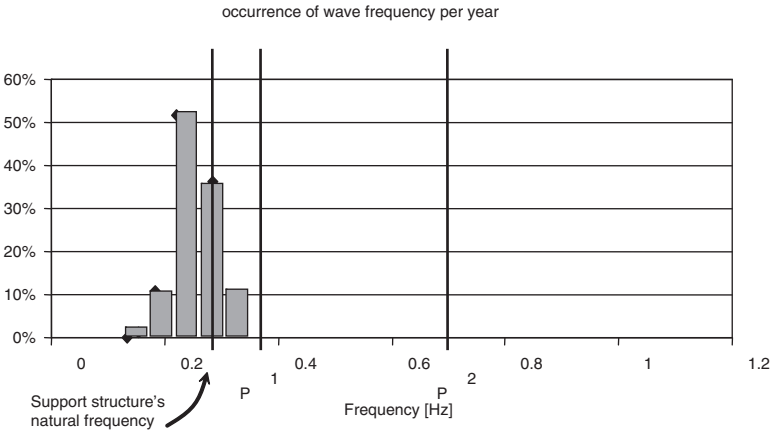

Figure 4: Rotation (1P) and blade passing frequency (2P) of the Opti-OWECS turbine with the structure's natural frequency and a histogram of the occurring wave frequencies.

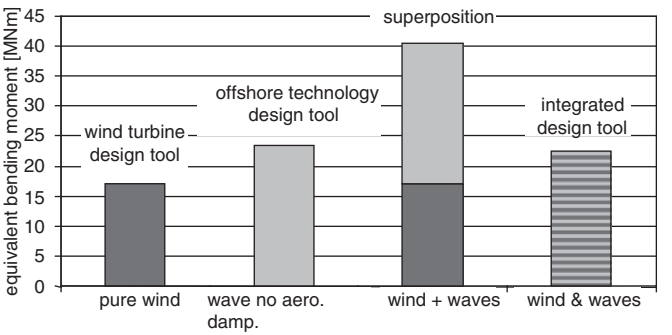

Figure 5: Comparison of fatigue calculations for wind only, wave only, wind and wave combines from separate and simultaneous analyses.

The fact that the structure's natural frequency coincided with a large portion of wave frequencies was further investigated. The aerodynamic damping of the turbine was found to reduce fatigue significantly, doubling the structures fatigue life when taken into account. To enable the analysis of this feature, full non-linear time domain simulations were found to be necessary of simultaneous wind and wave loading. Should wind and wave loads be analysed separately, the effect will not become visible by just adding the separate analyses as can be seen in Fig. 5.

Next to the detailed investigation of the dynamic behaviour in the design, a large number of practical issues were addressed in an integrated way. For installation it was found that onshore pre-installation would cause large cost reductions. For the correction of misalignment of the driven foundation pile, a transition piece was proposed. Installation of fully operational turbines and the misalignment correction are shown in Fig. 6. It was concluded that large-scale offshore wind

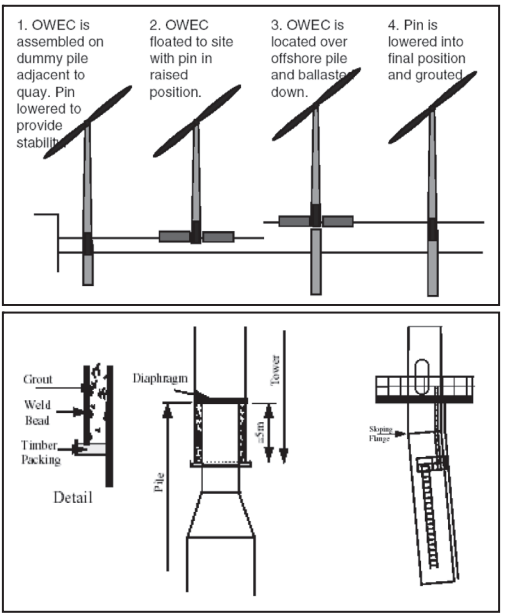

Figure 6: Installation of fully operational turbine and connection details between foundation pile and tower with misalignment correction.

energy application would require purpose-built vessels because existing vessel were either too large (offshore cranes) or too small.

2.2 From theory to practice: Horns Rev

The installation of Horns Rev in 2002 was the largest practical test of all theoretical findings. The installation of the foundation pile was done on a rather traditional manner: a small jack-up with a crane. For the installation of the turbines however two ships were entirely converted to purpose-built turbine installation vessels. Choosing a normal ship would ensure high sailing speed from and to port. A jacking system was added which only pre-stressed the legs without lifting the entire vessel out of the water. Two blades were already connected to the nacelle before placing it on the deck of the installation vessel. The method was christened "bunny ears" for obvious reasons. The installation of the tower and turbine was reduced to four lifts; two tower sections, nacelle with two blades and the final blade.

All appurtenances were pre-fitted in port to the transition piece: boat landing, J-tube, platform and the transition piece was grouted to the foundation pile. Figure 7 shows the "bunny ears", the A2Sea installation vessel, the transition piece being pre-fitted with a J-tube and the installation of the transition piece.

The design for the support structures on Horns Rev was fully covered by the owner of the wind farm: Elsam supplied all contractors with a complete pre-design, which was to be prized and for which an installation method was to be drafted.

Figure 7: Bunny ears, the pre-fitting of two blades, purpose-converted installation vessels, pre-fitting of J-tube to the transition piece and the installation of the transition piece.

Figure 8: Heli-hoist platforms are installed on turbines to lower mechanics for maintenance.

The design was well documented and integrated. The contractors were also invited to give their own alternative design. The amount of information for this part however was much less: the support structure was to end at 9 m above the mean sea level and the only interaction from the turbine was a static load and moment at this 9 m level. This did not improve integrated design but it can be argued that no contractor at that time would have any time for more detailed integrated turbine–foundation interaction analysis as all engineering went into "getting the things there".

For maintenance all nacelles are equipped with a heli-hoist platform onto which mechanics can be lowered even when boat access is not possible due to high waves (see Fig. 8).

The Horns Rev project proved that many practical issues addressed in the paper studies were applicable in real offshore wind. The amount of overall integration, or even the need for it is not crystal clear: many individual optimisations could be done without affecting the entire system.

2.3 Theory behind practice

The installation of the two turbines offshore of Blyth in the UK was part of a large EU-funded project to study Offshore Wind Turbines at Exposed Sites (OWTES).

One of the turbines is fitted with a complete measurement system to record external conditions and structural response. A picture of the turbines and the measurement systems is shown in Fig. 9.

The measurements were used to validate the current design tools for offshore wind turbines. It was found that present-day tools are very able to model the offshore wind turbine behaviour induced by wind and waves simulations. Figure 10 shows the comparison of measured and modelled mudline bending moment per wind speed.

It was found that offshore wind turbine design is very dependent on site-specific features like the wind and wave climate. At Blyth the local bathymetry is such that

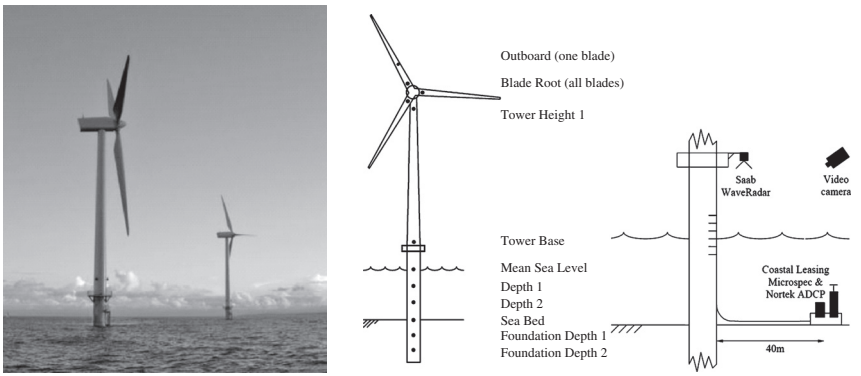

Figure 9: Turbines at Blyth with complete measurement system for external loads and responses.

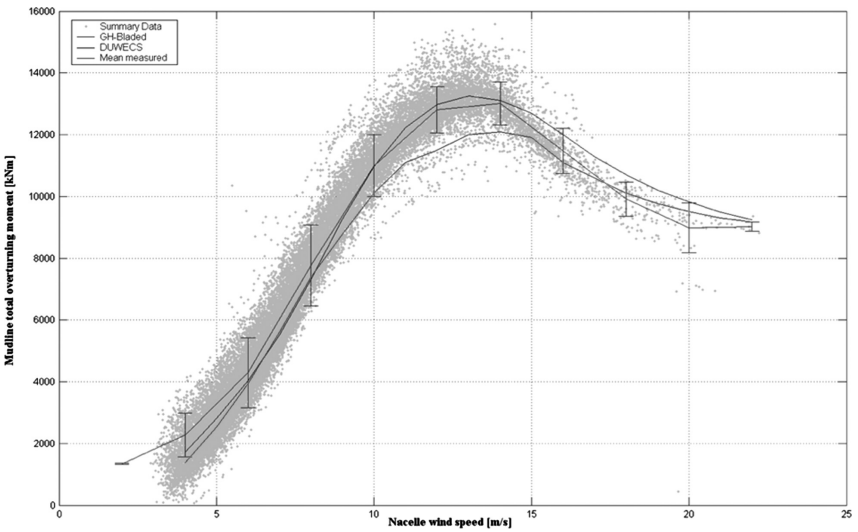

Figure 10: Comparison of mudline bending moment form measurements and modelling.

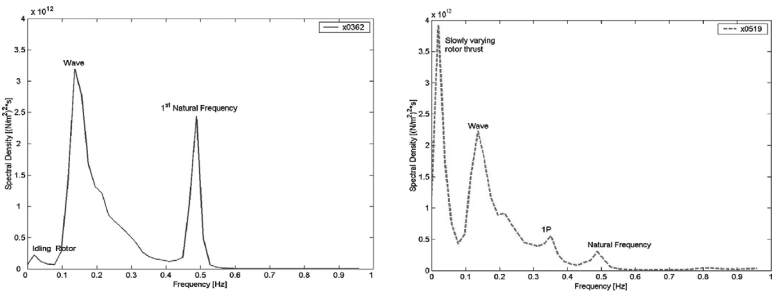

Figure 11: Response spectrum for mudline bending stress for idling (left) and operating (right) turbine.

near the turbines breaking waves are a common phenomenon. Although their influence did not affect the design dramatically in this particular case, they prove the importance of taking all details of a site into account.

Although the natural frequency of the structure is rather high at 0.48 Hz, the effect of both wind and wave loading on resonance is significant, as is the aerodynamic damping. Figure 11 shows the response spectrum for the mudline bending stress for equal environmental condition with an idling rotor (left) and a turbine in operation (right). The significant resonance peak in the wave-only case is damped dramatically when the turbine is operating.

From the measurements at Blyth it can be concluded that current modelling techniques are able to represent the critical features of offshore wind turbines properly, especially when on hindsight all structural and environmental parameters are known. It has also been shown that monopile structures are very dynamically sensitive, even in this case with relatively high natural frequency and that therefore proper analysis of resonant behaviour and aerodynamic damping deserve special attention.

3 Support structure concepts

3.1 Basic functions

The basic function of the support structure is to keep the wind turbine in place. This means that it has to be built to withstand loads originating from sea currents, waves and wind – acting on both the support structure and the turbine in operation.

A variety of wind turbines is available on the market, designed by different turbine manufacturers, in a range of power ratings. Each wind turbine has different characteristics. The offshore environmental conditions may also vary from site to site. Therefore, support structures are designed specifically for each case. It is not uncommon for one offshore site to have several variations of one type of support structure for one type of turbine.

The cost of the support structure on average amounts to around 25% of the total offshore wind turbine cost [1].

Typically the support structure is divided in two main parts:

1. The turbine tower
2. The foundation

The turbine tower normally consists of two or three sections. The design of the tower is usually provided by the turbine manufacturer. The tower is often installed in the same shift as the nacelle and the rotor.

The term foundation here refers to the turbine support structure, excluding the tower. It is essentially located below and at the water level. The function of the foundation is to direct the loads on the support structure into the seabed.

Many types of foundation for offshore wind turbines already exist. Essentially, the manner in which they are connected to the seabed determines how they are classified. The choice of foundation type depends primarily on the local water depth at the proposed site.

3.2 Foundation types

3.2.1 Monopile

The most frequently used foundation type is the monopile. It commonly consists of a foundation pile and a transition piece, on top of which the turbine tower is placed, as shown in Fig. 12.

Foundation piles are made from steel plates which are rolled and welded together to form a cylindrical section. The conventional method of installation (see Fig. 13)

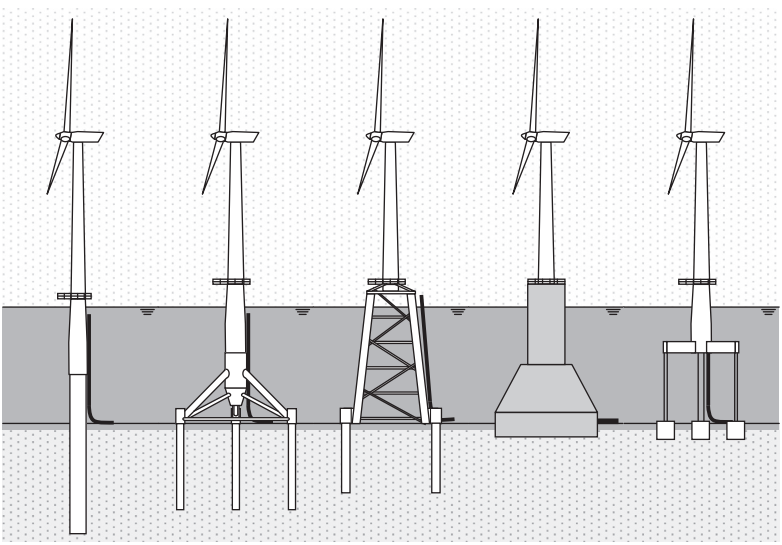

Figure 12: Foundation types, from left to right: monopole, tripod, jacket, GBS, floating.

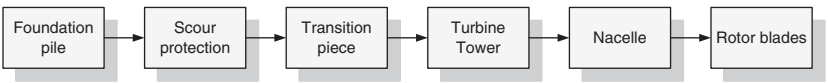

Figure 13: Installation sequence of main components for a monopile foundation.

Figure 14: The J-tube through which the power cable is directed to the seabed.

is by pile driving, whereby the foundation pile is driven into the seabed using hydraulic hammers.

If a foundation pile is designed to be driven into the seabed, a transition piece is required for the secondary structures such as J-tubes, boat landings and platforms as shown in Fig. 14.

If the seabed consists of rock, a borehole is prepared (drilled) in which the foundation pile is inserted. Since the foundation does not have to be designed for the impact forces of pile driving, the secondary structures can be attached directly to the foundation pile. Hence, no transition piece is needed.

Water currents flowing around the pile can, through erosion, create a depression in the seabed around the base of the pile, known as scour. The effect of scour on the foundation pile is as if it is positioned in deeper water with reduced soil-penetration depth. The depth of a scour hole depends on local currents and soil conditions, which is why it cannot be predicted accurately. Furthermore, an increased section of the pile is exposed to hydrodynamic loads. The increased length of the unsupported structure above the seabed may also result in a more dynamic behaviour.

To avoid scour, monopiles are provided with *scour protection*. Protection against scour is usually done by placing a "filter" layer of small stones around the pile. On top of that a layer of larger stones is positioned. The small stones keep the sand around the pile in place and the large stones keep the filter layer in place.

The relatively simple production and installation, together with the large range of exploitable water depths, have made the monopile the most widely used support structure concept. Its popularity has led the monopile to be developed for increasingly deeper waters. Monopiles are therefore likely to remain the most popular foundation type in the near future.

3.2.2 Tripod

A tripod foundation is a structure with three legs which diverge from a single node to their respective positions on the seabed. A foundation pile is driven into the ground at the base of each leg of the tripod section. On top of the tripod section, the turbine tower is placed. The procedure is visualised in Fig. 15.

Complications with production and installation make it relatively expensive. The main transition node where the three legs meet the central column is sensitive to fatigue. Stiffness benefits are only interesting in large water depths, but then the base becomes restrictively large.

The conventional installation method is to load several tripods onto a barge which is towed to the offshore site as depicted in Fig. 16. At a predetermined location, a structure is lifted of the barge, using a large crane (on the barge). Simultaneously, a smaller crane guides the tripod to its final position. The loads on the tripod

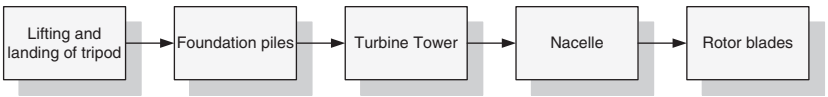

Figure 15: Installation sequence of main components for a tripod foundation.

Figure 16: Tripods on a barge, on their way to the Alpha Ventus wind farm.

structure will be mainly in axial direction. Therefore, scour protection is generally not required.

3.2.3 Jacket

Jackets, also known as space-frames or truss-towers, are relatively complex steel structures. Despite a reduction in construction materials (and hence weight), jackets are relatively expensive.

At the water depth where monopiles become uneconomical, jackets take over. However, due to ongoing developments, the monopile concept is used for increasingly deeper waters and the application of jackets is shifted to even deeper waters. For installation, a method similar to the one for tripods is applied (see Fig. 17).

3.2.4 Gravity-based structures

As the name implies, a gravity-based structure (GBS) utilizes the earth's gravitational force to stabilize its position.

GBSs usually have reinforced concrete foundations, referred to as caissons, in which a tower is placed. An example of GBSs for offshore wind turbines is shown in Fig. 18. Such GBSs are a proven technology for shallow waters. Occasionally they are used in deeper waters. The offshore wind farm Thornton Bank off the coast of Belgium applied reinforced concrete GBSs for a water depth of approximately 28 m.

Deeper waters require constructions with larger footprints in order to absorb greater moments. The increase of mass with water depth follows an approximately

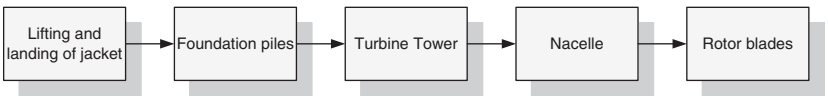

Figure 17: Installation sequence of main components for a jacket foundation.

Figure 18: GBSs for Thornton Bank, off the coast of Belgium.

quadratic relation. So even though building with concrete appears an economic choice, the large amounts required will make the structure relatively expensive.

An advantage with respect to installation is that a GBS can be floated out to its offshore location. A disadvantage is the necessary preparation of the seabed, which is done to provide the structure with a stable, horizontal floor. Another drawback is that, due to the great weight of the GBS, heavy lifting vessels are needed to perform the installation. The conventional installation sequence is shown in Fig. 19.

3.2.5 Floaters

The maximum water depth of wind farms has been steadily increasing over the last decade. Although monopiles will likely continue to be the most applied support structure for years to come, deeper waters appear to favour jacket structures.

Floating structures are seen by many as the solution to place wind farms in deeper waters (>70 μ). To keep it in place, the floating substructure is attached to the seabed through cables. In terms of installation costs, the question is whether such a system will require new installation procedures and dedicated vessels, or if it can simply be pre-assembled and transported by standard tugs (see Fig. 20).

4 Environmental loads

4.1 Waves

When calculating wave loads different wave categories can be distinguished, regular waves and irregular waves. Regular waves are periodic in nature and are usually associated with extreme load events. Irregular waves have a random appearance and are related to normal sea conditions and as such are to be adopted for fatigue evaluations.

For both regular and irregular waves several wave theories exist that allow the calculation of wave particle kinematics: the orbital motion, velocity and acceleration of infinitesimal quantities of water beneath the surface of the waves. Linear wave theory is valid for waves with infinitely small amplitudes, whereas non-linear wave theories are required for finite amplitude waves. Non-linear waves have a different surface profile compared to linear waves, with sharper, higher crests and longer and shallower troughs. Figure 21 shows which wave theory applies under

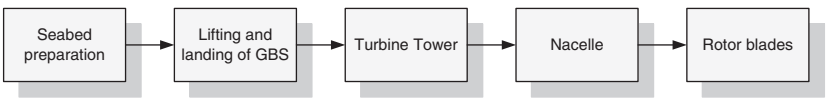

Figure 19: Installation sequence of main components for a GBS foundation.

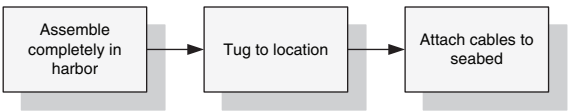

Figure 20: Proposed installation sequence for floating turbines.

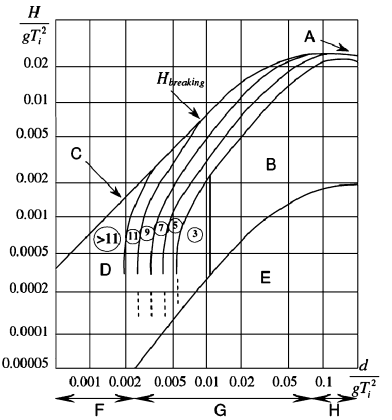

Figure 21: Range of application of various wave theories.

certain depth and wave steepness conditions. It can be seen that linear Airy wave theory can be applied in deep water waves with small steepness. Beyond this region non-linear wave theories such as Stokes' 5th order and stream function waves apply. This region in turn is limited by the wave breaking limit. In shallow water waves cannot grow higher than 0.78 times the water depth, while in deep water a wave will break if it grows too steep, with the wave height exceeding 0.14 times the wave length.

Linear Airy wave theory considers the surface elevation to be described by a harmonic wave:

$$\eta(x,t) = a\sin(\omega t - kx) \tag{1}$$

Using potential theory and boundary conditions at the seabed and at the free surface a velocity potential Φ can be formulated corresponding to the surface elevation described as in the following equation:

$$\Phi(x,z,t) = \frac{\omega a}{k}\frac{\cosh k(h+z)}{\sinh kh}\cos(\omega t - kx) \tag{2}$$

In this equation the term $\cosh k(h+z)/\sinh kh$ is the exponential decay function that describes the decrease of the intensity of the kinematics with increasing depth. By differentiating the velocity potential with respect to x and z the horizontal velocity u and the vertical velocity w can be derived, respectively, as follows:

$$u = \omega a\frac{\cosh k(h+z)}{\sinh kh}\sin(\omega t - kx), \quad w = \omega a\frac{\sinh k(h+z)}{\sinh kh}\cos(\omega t - kx) \tag{3}$$

The accelerations can be determined by differentiation of the horizontal and vertical velocities with respect to t.

$$\dot{u} = \omega^2 a \frac{\cosh k(h+z)}{\sin h\, kh} \cos(\omega t - kx), \quad \dot{w} = \omega^2 a \frac{\sinh k(h+z)}{\sinh kh} \sin(\omega t - kx) \tag{4}$$

As the above formulations are based on linear wave theory, assuming small amplitude waves, the kinematics can only be calculated up to the still water surface. To allow for the calculation of the kinematics up to the instantaneous water surface elevation some kind of extrapolation is required. Several methods exist of which Wheeler stretching is the most common. Up till now the origin was assumed to be in the still water line, with the negative x-axis directed downward. By applying Wheeler stretching, the negative x-axis is stretched or compressed such that the origin is in the instantaneous water surface, yet intersects the seabed at the same z coordinate as the original z-axis. To this end a computational vertical coordinate z' is used that modifies the original coordinate z with the use of the dimensionless ratio q, which is dependent on the water depth h and the surface elevation ζ. Using Wheeler stretching therefore implies that the kinematics are calculated at an elevation z as if it is at an elevation z' :

$$z' = qz + h(q-1), \quad \text{with q} = h/(h+\zeta) \tag{5}$$

Using the formulations for the wave kinematics the wave loads on a structure can be computed. This can be done with the help of Morison's equation. This equation assumes the wave load to be composed of a drag load term and of an inertia load term. The drag term is dependent on the water particle velocity whereas the inertia term is induced by the accelerations of the fluid. Equation (6) shows how the Morison equation can be used to calculate the wave force on a cylindrical segment of unit height and a diameter D:

$$F(t) = \tfrac{1}{4}\pi \cdot \rho \cdot C_{\mathrm{M}} \cdot D^2 \cdot \dot{u}(t) + \tfrac{1}{2} \cdot D \cdot C_{\mathrm{D}} \cdot u(t) \cdot |u(t)| \tag{6}$$

From this equation it can be seen that the drag term is non-linear. Furthermore, due to the fact that the drag term is dependent on the velocity while the inertia term depends on the acceleration, the occurrence of the maximum drag force and the maximum inertia force are separated by a phase shift of 90°.

Apart from the velocity and the acceleration of the water particle kinematics, the total wave force is dependent on a number of other parameters: the density of the surrounding water ρ and the hydrodynamic coefficients C_{D} and C_{M}. The drag coefficient C_{D} varies from 0.6 to 1.6, depending on the roughness of the cylinder and the Keulegan Carpenter number KC, a measure for the ratio between the wave height and the cylinder diameter. The inertia coefficient C_{M} can attain values ranging from 1.5 to 2.15, again depending on roughness and Keulegan Carpenter number. It should be noted that C_{D} increases with increasing roughness, whereas C_{M} decreases with increasing roughness. Finally the water depth, the water level above the still water surface and scour depth also influence the total wave load. Finally, marine organisms will accumulate on the structure below the water surface, thereby creating a layer of marine growth on the structure. This leads to an effective increase of the diameter, resulting in higher loads on the structure. This effect can be taken into

account by adding twice the thickness of marine growth to the diameter of the member under consideration, without an increase in mass.

4.2 Currents

Sea currents may originate from a variety of sources. Friction of the wind with the water surface may lead to wind-driven currents. Tides also contribute to currents. Further sources of currents are density differences, due to temperature or salinity gradients, wind surge and waves.

Depending on the origin of the currents, the current is most pronounced at different depths. Wind-driven currents, for instance are felt strongest near the surface, while tidal currents may be stronger over the entire depth. Friction with the sea bed will result in a near-zero current velocity at the bottom. These effects require the use of different current profiles in different circumstances. While measurements may lead to accurate descriptions of the local current profile, in the absence of data standard current profile expressions can be used.

For subsurface currents the profile can be described by an exponential profile, which describes the decrease of the current velocity with increasing depth d from the current velocity $U_{\mathrm{c,sub}}$ at the surface to zero at the seabed [2]:

$$U_{\mathrm{c,sub}}(z) = U_{\mathrm{c,sub}}\left(\frac{d+z}{d}\right)^{1/7} \tag{7}$$

For wind induced currents the following description can be adopted:

$$U_{\mathrm{c,wind}}(z) = U_{\mathrm{c,wind}}\left(\frac{d_0+z}{d_0}\right) \tag{8}$$

In this equation $U_{\mathrm{c,wind}}$ is the wind induced current at the still water line and d_0 is a fixed depth at which the current is zero. If the local water depth is less than d_0 the current profile is cut off at the seabed. For water depths larger than d_0 the wind induced current is assumed to be zero for depths larger than d_0. Commonly used values for d_0 are 20 [2] and 50 [3].

For evaluation of the current loads only the drag term of the Morison equation is relevant, as the accelerations due to the variations in current velocity over can be neglected. Due to the non-linearity of the drag term, the current load cannot be evaluated separately from the wave load. For a correct evaluation of the total hydrodynamic load on a structure, the current velocity must be added to the wave particle velocity. As the direction of the wave particle velocity and the current velocity is opposite for half the wave cycle it is important to calculate the term u^2 as the velocity ($u_{\mathrm{wave}} + u_{\mathrm{current}}$) times its absolute value as shown in the following equation:

$$F(t) = \tfrac{1}{4}\pi \times \rho \times C_M \times D^2 \times \dot{u}_{wave}(t) + \tfrac{1}{2}\rho \times D \times C_D \times (u_{wave}(t) + u_{current}) \times \left|(u_{wave}(t) + u_{current})\right| \tag{9}$$

4.3 Wind

Figure 22 shows a wind speed profile for a certain point in time. From this figure a number of characteristics can be deduced. First, that the mean wind is stronger at higher altitudes than near the surface of the earth. This is caused by friction of the moving air with the terrain. The effect becomes less pronounced as the altitude increases. The resulting difference in wind speed over altitude is called wind shear. Secondly, it is evident that the actual wind profile is very irregular. The actual wind speed deviates from the mean wind speed and direction as a result of turbulence. These two phenomena will be discussed briefly.

There are two commonly used models to describe wind shear: the logarithmic profile and the power law. The logarithmic profile is given by eqn (10), while eqn (11) describes the power law [4]:

$$\overline{V}(z) = \overline{V_r} \frac{\ln\left(\frac{z}{z_0}\right)}{\ln\left(\frac{z_r}{z_0}\right)} \tag{10}$$

$$\overline{V}(z) = \overline{V_r}\left(\frac{z}{z_r}\right)^a \tag{11}$$

In Fig. 23 both the logarithmic profile and the power law are shown. It clearly shows the difference between both models.

While the above gives a description for the mean wind speed, in reality the wind is never a steady flow of air that can be described with only one parameter. Local disturbances in the airflow called eddies cause the instantaneous wind speed to fluctuate around a mean value. This phenomenon is called turbulence. A measure

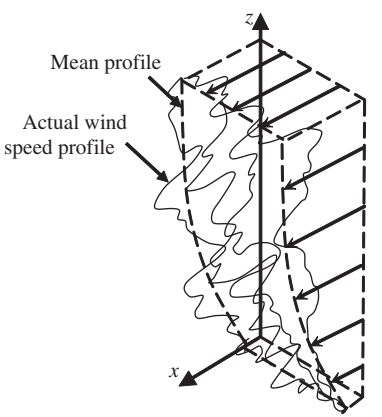

Figure 22: 3D turbulent wind velocity profile.

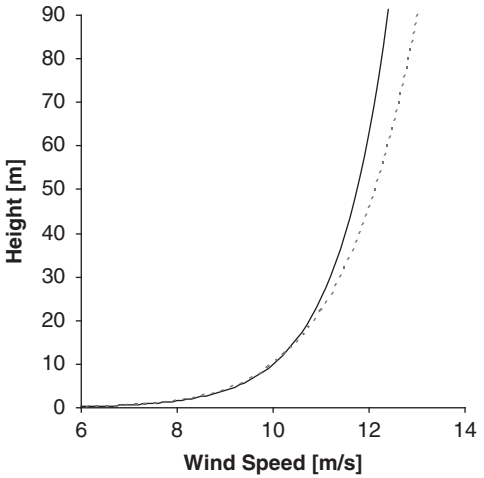

Figure 23: Wind shear profile according to logarithmic profile and power law.

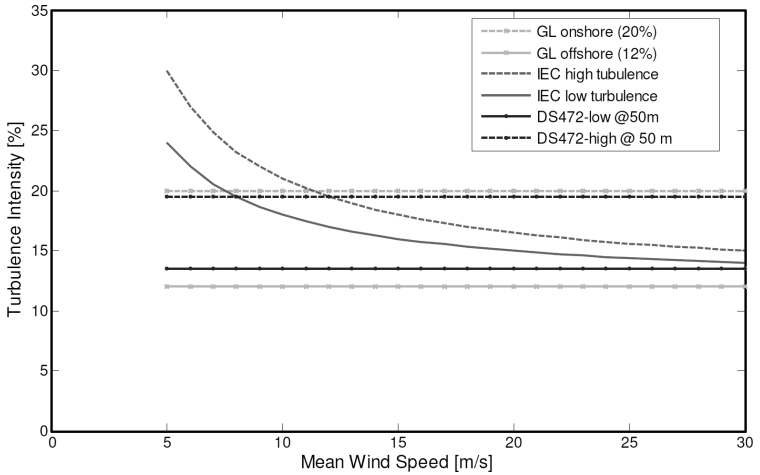

Figure 24: Various turbulence intensity models [4].

for the turbulence is given by the turbulence intensity I, which is defined as a function of the standard deviation and the mean wind speed as shown in the following equation:

$$I = \frac{\sigma}{V} \cdot 100[\%] \tag{12}$$

Recommended values for the turbulence intensity are given by various design standards. Figure 24 shows some turbulence intensity descriptions. It shows that the turbulence intensity is much higher onshore than offshore.

The wind loads on an offshore wind turbine can be split into operational loads on the turbine and loads on the structure. A description of the operational loads on the turbine and the load cases that should be considered can be found elsewhere in this work. The operational loads result in bending moments, normal forces and shear forces on the tower top.

The wind load on the tower structure itself results from drag forces only. To determine the total load on the tower structure the instantaneous wind speed should be evaluated at several elevations to account for wind shear. Subsequently, eqn (13) can be used to determine the drag force on each segment:

$$F_{tower}(t) = \tfrac{1}{2}\rho_{air} \cdot C_w \cdot D_{av} \cdot u^2_{wind}(t) \tag{13}$$

4.4 Soil

The soil contributes to the loading of the structure by providing the support reactions. In the case of piled foundations, these reactions are dependent on the lateral and axial pile–soil interaction. For GBSs the support reactions are generated by the vertical bearing capacity and the resistance against sliding.

Soil is generally a granular material, either cohesive such as clay, or non-cohesive such as sand. Other soil types that may be encountered are gravel, silt and peat. Soil originates either through erosion of rocks or through accumulation of organic material. Due to its geological history soil is highly inhomogeneous. The inter-particle voids are filled with water which may prevent or slow deformations [5].

The characterisation of loose to dense sand and soft to hard clay only gives a first indication of the ability of the soil to carry load. For design, more detailed knowledge is required. This is usually gathered through in-situ sampling and analysis of drilled samples in the laboratory. The first property measured for all types is the density ρ_{soil} (kg/m^3), usually for submerged soil, which is the dry density minus the density of water. A typical value is between 400 and 1000 kg/m^3. For clay, the undrained shear strength s_{u} and the strain at 50% of the maximum stress ε_{50} are measured. Table 1 gives an overview of typical values when no reliable soil data is available [4].

For sand the friction angle ϕ' and the relative density of sand D_{r} are derived directly from in-situ measurements. The initial modulus of horizontal subgrade reaction, k_{s}, can then be found with the graph in Fig. 25 [6].

Table 1: Characteristic parameters for clay.

Clay type	s_{u} (kPa)	ε_{50} (%)
Soft	0–25	1.5
Firm	25–50	1.5
Stiff	50–100	1.0
Very stiff	100–200	0.5
Hard	>200	0.5

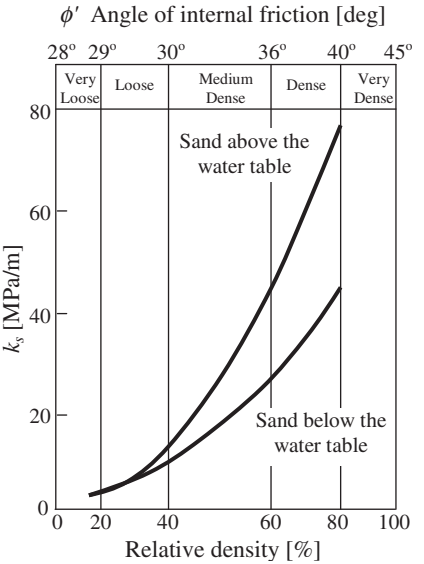

Figure 25: Initial modulus of subgrade reaction k_s as a function of friction angle ϕ' [6].

Due to its discontinuous nature soil particles can move with respect to the surrounding particles, thereby altering the structure of the soil. This creates a significantly non-linear behaviour which is usually described in terms of load displacement diagrams.

For a single pile in soil the pile–soil interaction can be described in terms of lateral resistance, shaft friction and end bearing. This behaviour is commonly modelled as non-linear load displacement curves: *P*–*y* curves for the lateral resistance and *t*–*z* and *Q*–*z* curves for the shaft friction and the end bearing respectively. Figure 26 shows *t*–*z* curves for sand and clay [6].

To model the soil reaction loads a set of soil springs is used. Figure 27 shows the springs for the horizontal and vertical direction as well as for the pile plug [4].

5 Support structure design

5.1 Design steps

The design of the support structure is an iteration between tuning the dynamic properties, optimising the amount of steel needed to resist all load cases and recalculating the loads on the optimised structure. Figure 28 shows the design steps that are typically required to come to a complete design of a support structure.

The different design steps have a strong interdependence and several iteration steps are normally required to come to an optimal design. For an entire offshore wind farm, some design details can be fixed. For instance, the hammer for installing

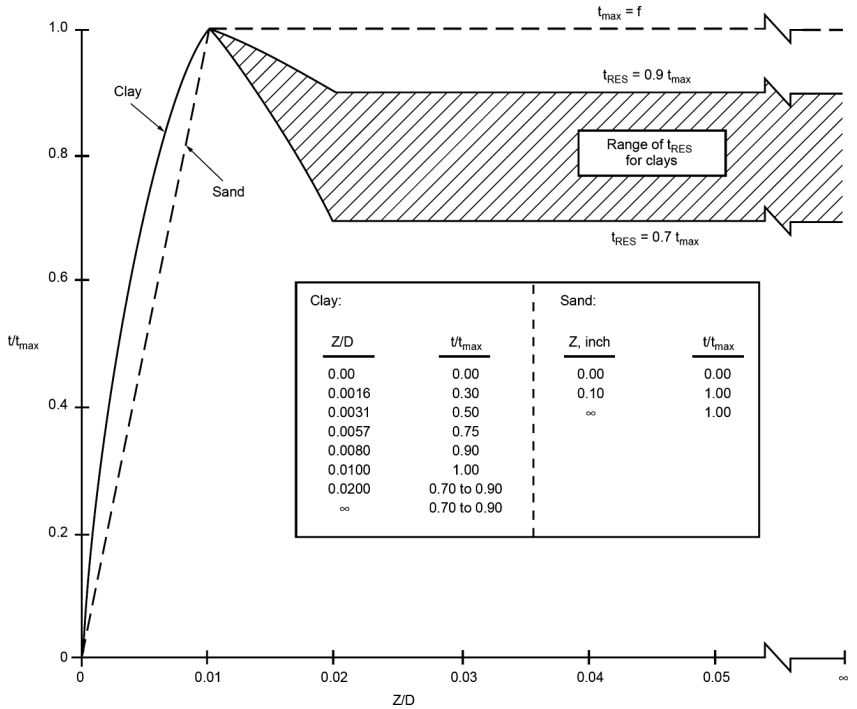

Figure 26: Load-displacement curves [6].

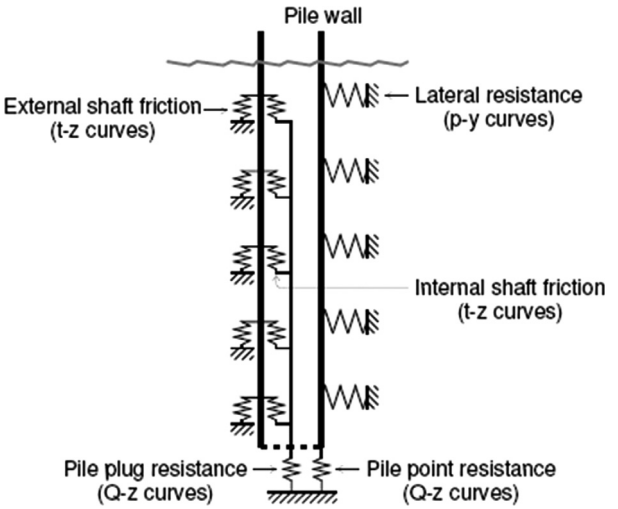

Figure 27: Modelling of pile–soil interaction [4].

the foundation piles can be of a single diameter, giving the designer less parameters to optimize.

In the previous chapter, the determination of design loads was treated. This chapter describes the steps to process this data and the turbine characteristics to come to a design of the structure.

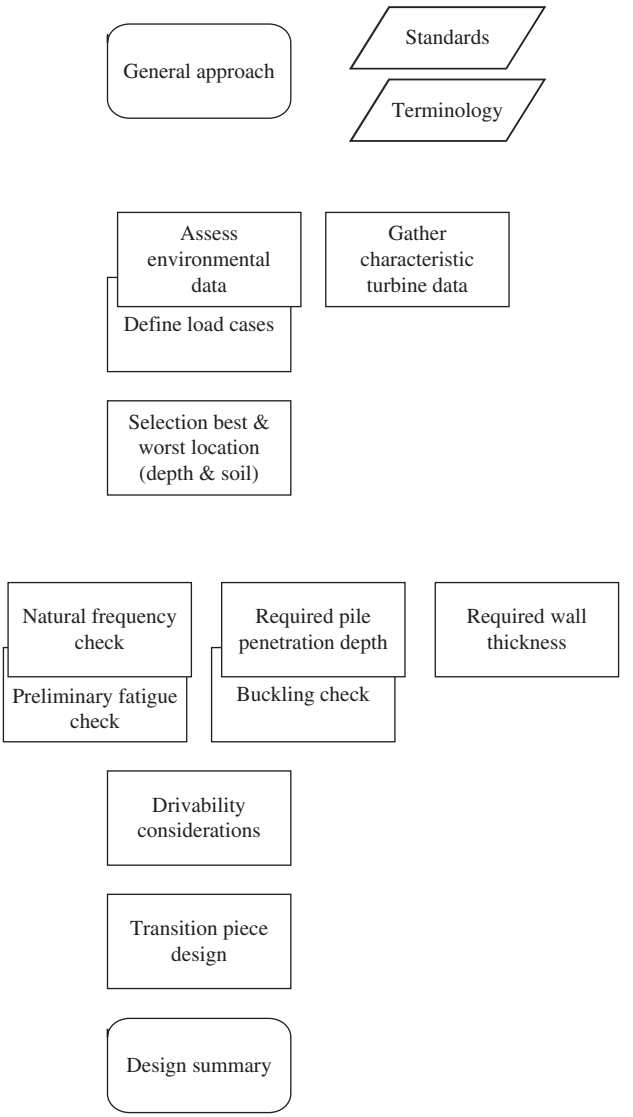

Figure 28: Design steps to come to a support structure design.

5.2 Turbine characteristics

The support structure has one main purpose: to keep the turbine up in the wind, where it produces energy. Wind turbines are fatigue machines by principle: with a rotation every 3 s on a desired availability above 98% per year for 20 years, a total of 200 million cycles. It is therefore key to design the support structure in such a way that the turbine dynamics and the support structure dynamics to not coincide.

Table 2: Turbine data.

	SWT 3.6 MW	V90 3.0 MW
Rotor		
Type	Three-bladed	Three-bladed
Diameter (m)	107	90
Swept area (m^2)	9000	6362
Turbine		
Minimum rotor speed (rpm)	5	8.6
Maximum rotor speed (rpm)	13	18.4
Blades		
Blade length (m)	52.0	44.0
Generator		
Nominal power (kW)	3,600	3,000
Tower		
Tower diameter (m)	3.051–5.000	2.300–4.200
Tower wall thickness (mm)	21–30	14–26
Operational data		
Cut-in wind speed (m/s)	4.0	4.0
Nominal power at approximate wind speed (m/s)	13.0	15.0
Cut-out wind speed (m/s)	25.0	25.0
Masses		
Nacelle + rotor mass (ton)	225	111

From the publically available turbine data, the required properties for support structure design can usually be gathered:

- turbine rotation speed range
- number of blades
- tower height
- turbine mass

Table 2 shows details for two commonly used turbine types.

5.3 Natural frequency check

From the turbine characteristics, the frequency ranges for the design of the support structure can be determined. The natural frequency of the structure should not coincide with the rotor speed range (1P) and blade passing speed range (3P for three-bladed turbines).

A first-order calculation of the natural frequency of a structure can be performed with the following simplified model. When the support structure is modelled as a mass on pole with the mass being the turbine mass and the pole a single diameter and wall thickness steel pile as depicted in Fig. 29.

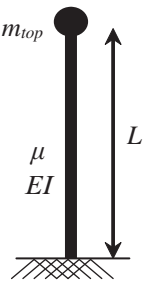

Figure 29: Structural model of a flexible wind turbine system.

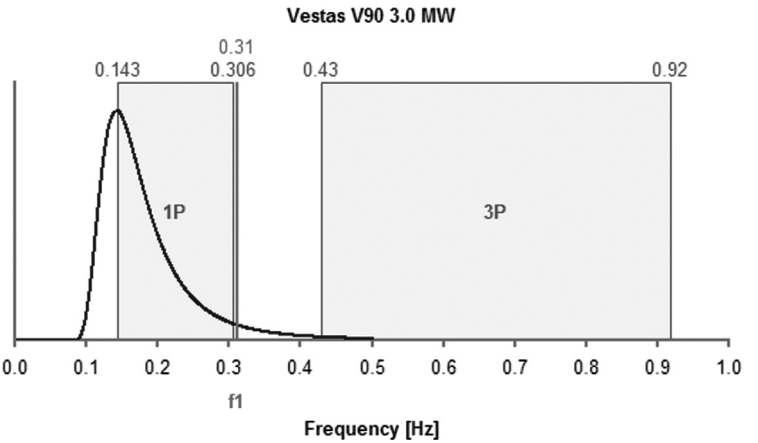

Figure 30: Frequency areas of 1P and 3P for the V90, with the designed natural frequency at 0.31 Hz between 1P and 3P to prevent dynamic interaction.

For this model consisting of a uniform beam with a top mass and a fixed base, the following approximation for the calculation of the first natural frequency is valid:

$$f_{\text{nat}}^2 \cong \frac{3.04}{4\pi^2} \frac{EI}{(m_{\text{top}} + 0.227\mu L)L^3} \tag{14}$$

with f_{nat} is the first natural frequency (Hz), m_{top} the top mass (kg), μ the tower mass per meter (kg/m), L the tower height (m) and EI is the tower bending stiffness (N m^2).

The 1P and 3P areas can be plotted in a figure to visualize the zones in which the support structure natural frequency should not lie. In Fig. 30 this is shown for the V90 from Table 2 in the previous section.

The natural frequency will change through the next steps of design. It will need to be checked against this diagram to make sure it falls within the area between 1P and 3P.

For more detailed determination, the natural frequency will of course be calculated using a finite element model of the structure.

5.4 Extreme load cases

The main parameter resulting from the natural frequency check is the pile diameter. For the part of the support structure that is submerged, the diameter determines the hydrodynamic loads: waves and currents. The extreme load cases on an offshore wind turbine and the soil reaction to support those loads are shown in Fig. 31.

The rest of the loads are aerodynamic loads on the turbine and the tower. The combinations of these loads under different conditions are prescribed in the design standards. To take the probability of occurrence into account, several load combinations are prescribed: maximum 50-year wave load combined with a reduced 50-year gust event and the reduced maximum 50-year wave load combined with the full 50-year gust. An overview of load combinations is shown in Table 3.

5.5 Foundation design

Now that the global structural dimension and the design load cases are known, the foundation design can be detailed.

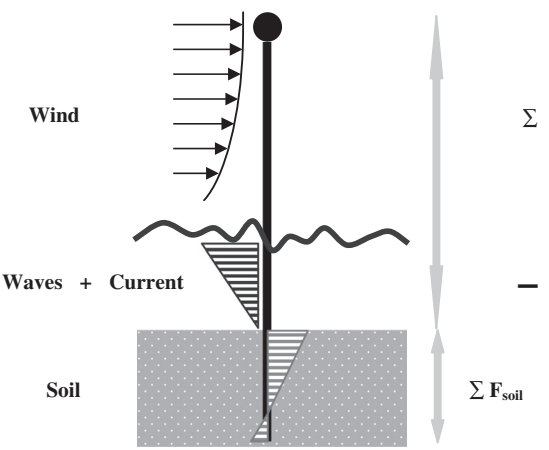

Figure 31: Extreme load cases on the offshore wind turbine and the soil reaction to support those loads.

Table 3: Load combinations [3].

		Environmental load type and return period to define characteristic value of corresponding load effect				
Limit state	Load combination	Wind	Waves	Current	Ice	Water level
ULS	1	50 years	5 years	5 years		50 years
	2	5 years	50 years	5 years		50 years
	3	5 years	5 years	50 years		50 years
	4	5 years		5 years	50 years	
	5	50 years		5 years	50 years	

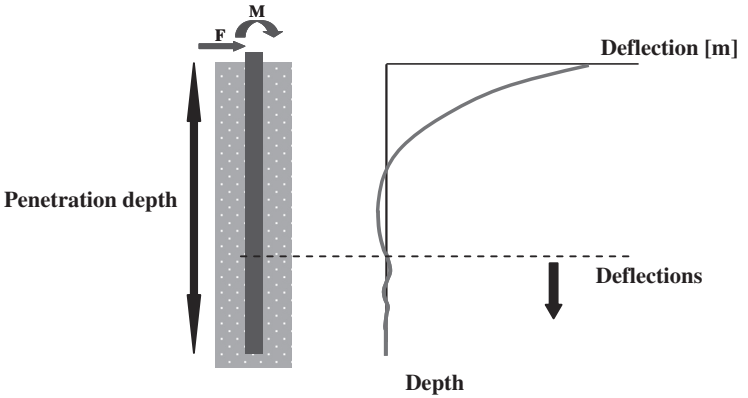

Figure 32: Pile deflection.

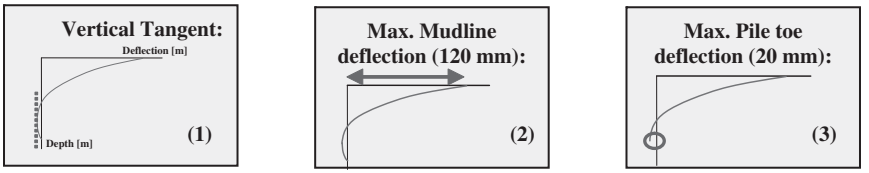

Figure 33: The three checks for foundation pile length design: vertical tangent at the pile toe, maximum deflection at the mudline, and maximum toe deflection.

The foundation pile can be modelled separately in a program incorporating detail soil models following the *p–y* method described in the previous chapter. The deflection of the pile is shown in Fig. 32. To start the pile penetration depth design, a pile length of seven times the pile diameter is chose to be sure the pile tip deflection is negligible.

With the foundation pile modelled in the finite element program, the pile length can be reduced while the following three checks are monitored after each step (Fig. 33):

1. the pile tip should reach a vertical tangent
2. the deflection of the pile at mudline is less than 120 mm
3. the deflection at the toe is less than 20 mm

5.6 Buckling & shear check

Now that the foundation pile has been modelled, also the pile–soil interaction is known and the deflection of the structure under different loads. The structural steel can now be checked for integrity under extreme load cases.

5.7 Fatigue check

The biggest step in optimising the design of the support structure is checking the fatigue. Fatigue is the phenomenon of slow deterioration of the steel due to

continuous varying loads over time. For a fatigue check it is therefore vital to know the following details:

- environmental loads over the lifetime of the structure
- steel properties at the most severely loaded sections (typically: welds)
- fatigue resistance of the details of these welds: empirical S–N curves.

The long-term environmental loads are usually gathered in tables listing the simultaneous occurrence of wave height, period and direction, wind speed and direction and potentially several other parameters. For the fatigue check of the support structure the amount of data for a 20-year lifetime can accumulate to over 1000 load cases. To reduce these for the initial design stages, scatter diagrams are used. Table 4 shows a typical scatter diagram for wave height and period.

Such a wave scatter diagram is available for every wind speed bin (0–2 m/s wind, 2–4 m/s, 4–6). We then have the simultaneous occurrence of wave height, period and wind speed in a 3D scatter diagram.

To calculate the fatigue of the structure, we ideally need to run all these load cases through a wind turbine simulation program such as Bladed or Flex to incorporate all wind, wave and structure interactions an find the stress variations in each critical point of the structure. In the preliminary design stages, a reduced amount of data can be used that represents the most commonly occurring wind and wave conditions. Typically, the amount of data is reduced to 15 or 20 of these environmental states. An example for the Blyth turbines is shown in Table 5.

Table 4: Wave scatter diagram for H_s and T_z with occurrence in parts per thousand for the OWEZ location.

H_s (m)	T_z (s)								Sum
	0–1	1–2	2–3	3–4	4–5	5–6	6–7	7–8	
6.5–7.0									0.0
6.0–6.5								0.1	0.1
5.5–6.0							0.1	0.1	0.2
5.0–5.5							0.1	0.1	0.2
4.5–5.0							1		1.0
4.0–4.5							4		4.0
3.5–4.0						4	5		9.0
3.0–3.5						19	0.1		19.1
2.5–3.0					0.1	38			38.1
2.0–2.5					27	43			70.0
1.5–2.0				0.1	115	5			120.1
1.0–1.5				6	220	1			227.0
0.5–1.0				236	145	1			382.0
0.0–0.5	1		1	113	14	0.1			129.2
Sum	1.0	0.0	1.0	355.1	521.1	111.1	10.4	0.3	1000

Table 5: Summary of 15 environmental states for Blyth.

	H_s (m)	T_z (s)	V_w (m/s)	% of occurrence
1	0.25	2.0	5.0	20.47
2	0.25	5.2	4.9	3.73
3	0.25	4.0	11.8	21.76
4	0.25	5.6	15.7	3.85
5	0.25	5.8	20.6	1.00
6	0.75	3.4	6.7	8.62
7	0.75	5.3	5.8	13.25
8	0.75	5.5	11.7	5.58
9	1.25	5.2	8.8	10.66
10	1.25	8.0	8.5	1.25
11	1.75	6.0	9.9	4.83
12	1.75	6.7	16.2	0.55
13	2.4	6.8	12.8	3.54
14	3.4	7.8	14.5	0.77
15	3.3	9.7	18.7	0.14
				100%

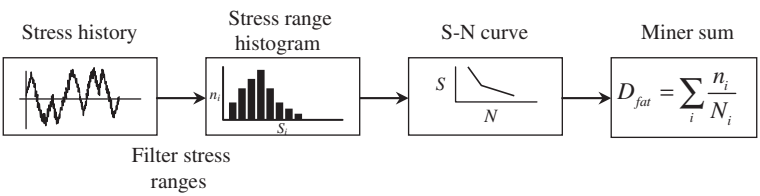

Figure 34: Flowchart of fatigue calculation due to variable stress ranges using *S–N* curve and Miner sum.

When the stress signal is determined for each location that needs to be checked, the fatigue calculation can be performed. Figure 34 shows the calculation steps: the stress history is converted to stress ranges via the rainflow counting method. The stress ranges are then checked against the *S–N* curve for the detail under consideration and the fatigue damage due to the load case is calculated using the Miner sum.

When the Miner sum is determined for each load case, it is multiplied by the percentage of occurrence during the design life of 20 years. The total fatigue damage is then found by adding the damage of all individual load cases together.

Should a detail not pass the fatigue check, changing the wall thickness will reduce the amount of stress and a re-calculation of the fatigue can be performed. To check the full fatigue of a monopile design requires several hours of computation time with current industry standard software. New methods of calculating the fatigue in the frequency domain show promising results and they have found their way to preliminary design calculations.

5.8 Optimising

The design steps described in this section have been treated on a high level only. The design process will involve several repetitions in which structural properties change in one step and require checking in all other steps again. Furthermore, some steps have not been treated here: the design of secondary steel and its impact on support structure loads and stress concentrations; the drivability analysis of the pile and the associated fatigue (the pile loses 25–30% of its fatigue resistance during installation); the impact of scour, corrosion and marine growth, etcetera.

6 Design considerations

6.1 Offshore access

The majority of the maintenance activities that are required during the entire lifetime of an offshore wind farm consist of simple repairs rather than the replacement of turbine parts. Therefore, the accessibility to be treated here will involve personnel and light equipment only. The accessibility of a wind turbine depends first of all on the chosen access method. In the offshore industry there are two means of transportation used to reach offshore structures: helicopters and vessels.

6.1.1 Helicopters

Helicopters are used regularly to gain access to various offshore installations since they provide a fast means of transportation for personnel and light equipment at cruise speeds up to 250 km/h. Another big advantage of using helicopters is that both travel and access operations are not limited by wave conditions. If an offshore structure is equipped with a helicopter landing deck, the helicopter can land on this deck and passengers can safely board or exit the helicopter. However, mounting a landing deck on an offshore wind turbine would be unpractical. Instead, a hoisting platform can be placed on the turbine nacelle. The transfer of personnel from helicopter to turbine is then achieved by having the helicopter hovering above the turbine and hoisting people from the helicopter down to the platform on top of the turbine. Although this method is fast, disadvantages are the high costs of operation and the fact that a hoisting platform is required on each turbine. In addition, most exploiting parties are not eager to use this method due to the risks involved using helicopters: in case of a crash, the risk of casualties is high. In fact, the Horns Rev wind farm, located in the North Sea 14 km west of Denmark, is the only wind farm where helicopter hoisting is applied as a means of access. Furthermore, this method only allows transferring personnel with a very limited amount of tools and safe flying can be hampered by limited visibility and too large wind speeds. The accessibility of a helicopter is therefore determined by the percentage of the time that both wind speed and visibility are outside the restricted values.

6.1.2 Vessels

The use of vessels is a more cost-efficient and probably safer way of accessing offshore wind turbines than using helicopters. Currently, the most commonly used

(*a*) (*b*) (*c*)

Figure 35: Ship-based access to offshore wind turbines. Ships used: (a) WindCat; (b) Aaryan; (c) Moidart.

vessels for wind farm support are small vessels with lengths between 14 and 20 m, with either a single or a twin hull shape, and a bow section that is designed for access. Safe access is provided by intentionally creating frictional contact between the vessel and a boat landing structure on and in order to have no vertical vessel motions at the point of contact. A rubber bumper on the vessel bow forms this contact point; the thrusters push the boat against the structure to create the friction. The boat now pivots around the bumper and personnel can step from the vessel bow onto the turbine ladder safely. This method is generally being used for maintenance visits and applied by different types of vessels as shown in Fig. 35.

This ship-based access to offshore wind turbines is limited by wave conditions. As wave conditions get rougher, ship motions will become lager and there is a possibility that the vessel loses its contact with the boat landing. As a result, the vessel can start moving relative to the offshore structure. In this situation, the safety of the person accessing the turbine can no longer be guaranteed: the access procedure is no longer safe. For this reason, access operations are limited to certain wave conditions. The general way of describing the limiting wave conditions for access is by giving the limiting significant wave height for an access method. In wave conditions exceeding this limiting significant wave height, the access operation is considered too dangerous and will therefore not be performed.

6.1.3 Motion compensation systems: Ampelmann and OAS

The core of the problem when transferring people from a ship to a structure is that the vessel moves with the waves and the structure is stationary. The development of offshore wind sparked new innovations in this field. Several systems have been developed that compensate the wave motions partially or fully to remove the relative motion problem. The Offshore Access System is a hydraulic gangway that compensates the heave motion while connecting to the offshore structure. The offshore structure needs to be equipped with a landing station where the OAS grabs onto. As soon as the contact is made, the active compensation is switched off and the gangway hinges passively on both ends, as shown in Fig. 36.

The Ampelmann follows a different approach: it cancels all motions in the 6 degrees of freedom (surge, sway, heave, roll, pitch, yaw) to achieve a completely stationary platform. A gangway is then extended that is lightly pressed against the structure to allow quick and safe access. The additional advantage is that no landing station is

Figure 36: Access to offshore structure with OAS.

Figure 37: Ampelmann system for accessing offshore wind turbines.

needed, saving steel on each single support structure. The Ampelmann is shown in Fig. 37.

Both systems allow safe transfer in sea states up to H_s = 2.5 m, enabling maintenance crews to access the turbines over 90% of the year.

6.2 Offshore wind farm aspects

In this chapter the design of support structures was the main theme. The support structures and their turbines make up the offshore wind farm. The design of the offshore wind farm as a whole also has impact on the single support structures. The most pronounced items are summarised here.

6.2.1 Wind farm layout

The offshore wind farm layout is first and foremost determined by the consented stretch of seabed available for the farm. But within this area, optimisation on farm level is possible. The first design goal is to place the turbines close to each other to limit cable length, and as far apart as possible to increase power capture.

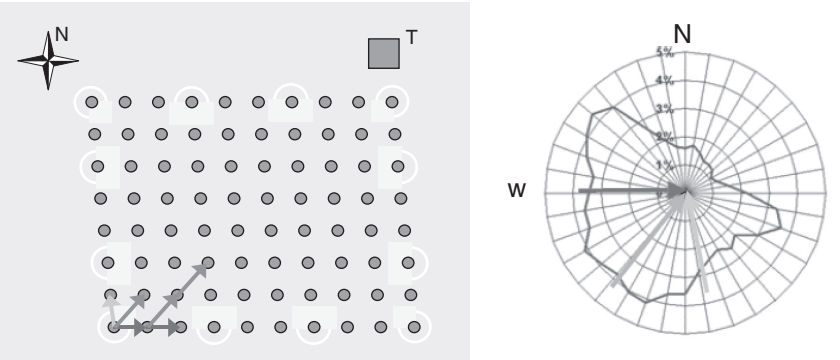

Figure 38: Wind farm layout with the wind rose on site.

Because the wind flow offshore is less turbulent, the mixing of the air behind the turbine (which has been slowed down due to the extraction of energy) takes longer to regain strength from the undisturbed wind around it. This means that turbines need to be placed further apart in offshore wind farms compared to onshore where turbulence intensity is higher. The rule of thumb is to place turbines at least seven times the rotor diameter apart. Smart layout configurations help increase the distance between the turbine in the governing wind direction to 10D or more, while maintaining the 7D minimum distance to make sure the cable length does not increase too much. Figure 38 shows such a layout with the wind rose on site.

6.2.2 Electrical infrastructure

The offshore wind power needs to be transported to the electricity grid. Within the offshore wind farm, in-field cables connect the turbines to each other. For most larger offshore wind farms (>100 MW) a transformer station is normally used. Here all in-field string cables come together. The total power is gathered and the voltage is increased to reduce losses to shore along the "shore connection cable". Typical voltages in fields are order of magnitude 33 kV, to shore 50 kV.

The in-field cable routing has influence on the design of the support structures: to most turbines two J-tubes will guide the incoming and outgoing cable, requiring secondary steel attachments that can add significant hydrodynamic loads. For installation purposes it can be very beneficial to choose a simple grid type of layout. Should a "star grid" or other, non-regular pattern be chosen, maintenance vessels may damage them in later years when there is confusion about the exact location.

6.2.3 The support structure in the offshore wind farm

Offshore wind farms are complex systems placed in a harsh environment, designed to operate on their own for large periods of time. The support structure is an integral

part of these systems and should be treated as such. The design steps depicted in this chapter give a first rough guide to finding an optimised solution. The detailed design of the support structure requires intense cooperation between the different disciplines involved in offshore wind farm design and construction. Only then can the true potential be unleashed of the force we know as "offshore wind".

References

[1] Ferguson, M.C., et al. (ed), Opti-OWECS final report Vol. 4: a typical design solution for an offshore wind energy conversion system, Institute for Wind Energy, Delft University of Technology, 1998.
[2] Germanischer Lloyd, *Rules and Guidelines for the Design of Offshore Wind turbines*, Hamburg, Germany, 2004.
[3] DNV, *Design of offshore wind turbine structures*, Det Norske Veritas, DNV-OS-J101, 2004.
[4] Tempel, J. van der, Design of support structures for offshore wind turbines, PhD. Thesis, Delft University of Technology, Section Offshore Engineering, 2006.
[5] Verruijt, A., *Offshore Soil Mechanics*, Delft University of Technology, 1998.
[6] API, *Recommended Practice for Planning, Design and Constructing Fixed Offshore Platforms – Working Stress Design*, American Petroleum Institute, 21st edition, 2000.